Ytterbium Luminescence and Up-Conversion

Introduction

Photoluminescence up-conversion (UC) occurs when an ion in its ground state is excited by a photon and subsequently transfers that energy to another ground state ion, through one or more photons. This phenomenon can take place both in organic and inorganic materials through mechanisms such as cooperative UC, via an antennae effect from organic ligands[4] in a lanthanide complex or ground-state absorption and excited state absorption (GSA/ESA).[7,8] By contrast, down-conversion (DC) is the process by which one high energy photon is converted to 2 or more lower energy photons through Stokes' emissions.[6] UC has largely been studied and applied to nanoparticles[6] and lanthanide doped lattices,[1] with only a handful of molecular UC devices reported.[2,3,5] Ytterbium-based systems are largely used, wherein Yb(III) acts as a sensitizing ion absorbing NIR radiation, allowing $^2F_{7/2} \rightarrow {}^2F_{5/2}$ excitation. This energy is then transferred through radiative pathways to neighbouring activator ions, which in turn emit photons in the visible light. Potential applications include security (multilevel anticounterfeiting)[6], biolabeling/bioimaging[9,10] and lighting technologies (e.g. field colour displays, UC lasers)[7,8].

The emission of light from a Ln^{III} ion is characterized by the excited state lifetime ($\tau_{obs} = 1/k_{obs}$) and the quantum yield, ϕ.

$$\varphi = \frac{\text{number of emitting photons}}{\text{number of absorbed photons}}$$

$$\varphi_{\text{Ln}}^{\text{Ln}} = \frac{k^{\text{rad}}}{k_{\text{obs}}} = \frac{\tau_{\text{obs}}}{\tau^{\text{rad}}}$$

The intrinsic quantum yield (ϕ) is the quantum yield of metal-centred luminescence upon direct excitation and reflects the extent of non-radiative deactivation processes, measuring the efficiency of photon emission. The rate constant, k_{obs}, is the sum of all deactivation processes, including vibration-induced and photo-induced energy transfers (ET). Yb(III) has a strong oscillator strength for the $^2F_{7/2} \rightarrow {}^2F_{5/2}$ transitions (i.e. high probability of absorption of EM radiation), a quantum efficiency of 1 and there are no intermediate energy levels between $^2F_{7/2}$ and $^2F_{5/2}$.

The current review integrates key aspects of modern literature concerning UC mechanisms in bulk solids and discrete molecular systems in solution, as well as highlighting potential applications, and the scope for further research.

Cooperative UC in host lattice systems

Heterogenous systems consisting of a sensitiser and one or more activators usually cannot be explained by a single UC mechanism, as extra variables result in competing mechanisms or additional dependencies. In a system of $SeCl_2$ host lattice doped with Yb:Tb, the sensitiser Yb^{3+} only has one excited state, $^2F_{5/2}$ of energy 10 000 cm^{-1} whilst Tb^{3+} does not have any excited states in this spectral region.[1] Two NIR photons are absorbed by 2 Yb^{3+} ions, which are subsequently and simultaneously transferred to the neighbouring Tb^{3+}. This energy transfer process allows the $^7F_6 \rightarrow {}^5D_4$ transition in Tb^{3+} to occur, ultimately leading to the green emission associated with the $^5D_4 \rightarrow {}^7F_6$ transition.

In this particular circumstance, a cooperative sensitisation mechanism can only occur at higher temperatures, where host phonons can contribute to UC-active ions. As the excited state of Yb^{3+} $^2F_{5/2}$ becomes thermally populated, ET can occur more readily. A phonon is a vibration of the atomic lattice. The higher the thermal energy of the atoms, the greater the vibrational energy. These vibrations then pass from one atom to another in the solid lattice. When the whole lattice vibrates as a wave at a single frequency, the vibration is called a phonon. When the temperature is too low to allow for phonons, the green emission from $^5D_4$ level of Tb^{3+} is no longer observable. Instead, Yb-Yb pair emission is visible, giving a blue light. Negatively, phonons provide non-radiative pathways, where overtones fill the energy gap between the ground and excited states in the activator ions, reducing emission intensity and lifetime.

In the formation of doped-lattice systems, the 'clustering effect' of rare earth metal ions may take place.[1] This effect occurs when chemical clusters of a few angstroms in size form during synthetic procedures. In these areas, ion-ion interactions of all kinds are substantially increased, due to shorter inter-ionic distances. Shorter distances allow for more efficient radiative transitions from sensitiser to activator ions. However, back energy transfers and self-quenching, as well as 'concentration quenching' may counteract

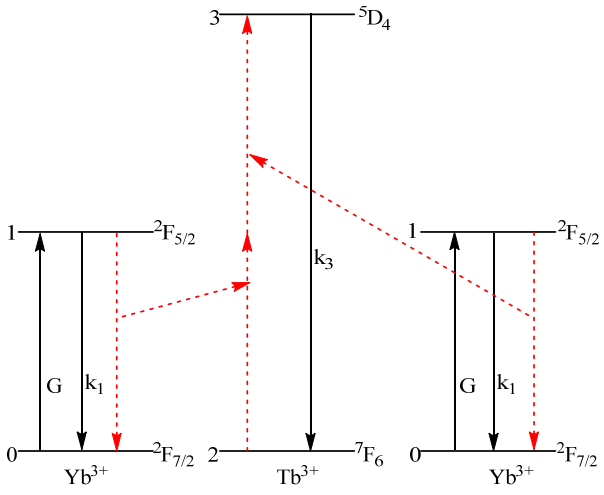

Figure 1: Cooperative sensitisation of Tb^{3+} by 2 excited Yb^{3+} ions. The solid arrows represent radiative transitions; dashed represent non-radiative ET.

that efficiency. 'Concentration quenching' occurs when ion-ion excitation energy is diffused throughout the sample, resulting in decreased emission intensity. In solution, better distance control between active centres and their gatherings can be achieved by varying the active ion concentrations.[2] This can potentially improve UC efficiency and partially counteract quenching arising from vibrational energy transfer to oscillators.[2,3,4,5]

UC Mechanisms in Molecular Systems

Longer luminescence lifetimes and higher quantum yields are sought after in UC mechanisms, both in solid lattice systems and discrete molecular devices. In order to increase efficiency in molecular systems, the dissipation of excited-state energy from sensitisers ('energy tanks') must be limited.

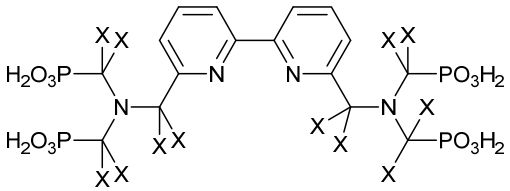

Figure 2: Structure of the perdeuterated tetraphosphonated bipyridyl ligand L^1.[2]

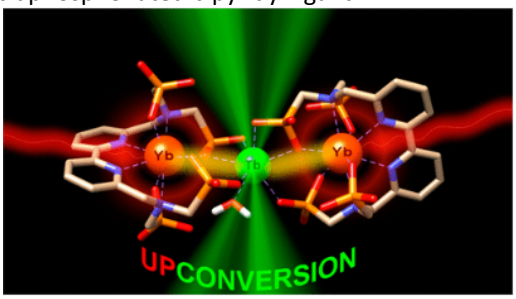

Figure 3: $[(YbL^1)_2\ Tb_x]$ where x = 1 to 3. $[(YbL^1)_2\ Tb]$ species showing red and green emission of Tb^{3+}.[3]

High energy vibrational oscillators, such as O-H, N-H, C-H, act as efficient excited-state quenchers. Such IR absorption bands are present in all solvents, as well as within ligands and ideally must be kept far away from absorbing and emitting centres. Perfluorinated or deuterated polydentate[2,4] ligands are therefore used, fulfilling the primary coordination sphere and protecting central lanthanide cations by blocking out solvent molecules. By exchanging H with either F or D atoms, the vibrational oscillation energy of the bonds decreases and no longer matches the Yb^{3+} $^2F_{7/2} \rightarrow {}^2F_{5/2}$ energy. This results in improved luminescence, higher Q.Y. and longer excited lifetimes.

Ligands like those in *Figures* 2-6 enclose the Yb cation in cage-like structures, providing good shielding from solvent molecules.

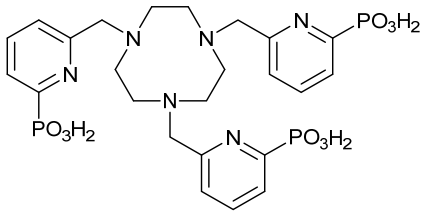

Figure 4: 1,4,7-triazacyclononane ligand with 3 pyridyl groups, L^2

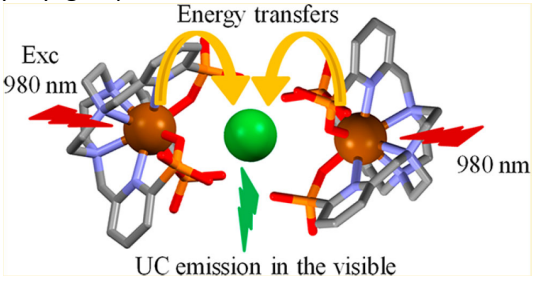

Figure 5: Phosphonate ligand present in heteropolynuclear complexes of $[(Yb(L^2))_2Tb_x]$ compositions (x = 1 and 2).[5]

$[(YbL^1)_2Tb_x]$ (*Figure 3*) is partially coordinated to a solvent molecule as L^1 has a smaller chelate bite angle than 1,4,7-triazacyclononane (L^2) ligand (*Figure 4*). The steric compression around the Yb^{3+} metal centres caused by the larger chelate bite angle in the aza-phosphonated ligands leads to decreased coordination numbers by exclusion of solvent molecules from the primary coordination sphere.[5] This results in a smaller quenching effect of Yb^{3+} and better ET from Yb to Tb for $[(Yb(L^2))_2Tb]$ than for $[(YbL^1)_2Tb]$.

The UC mechanisms involved in the species $[(Yb(tacn))_2Tb]$ and $[(YbL^1)_2$ Tb] are similar. The mechanism corresponding to $[(YbL^1)_2Tb]$ is cooperative photosensitized Energy Transfer Up-conversion (ETU) instead of GSA/ESA. GSE/ESU is highly unfavourable for molecular systems composed of an acceptor and one or more energy donors, because it requires large concentrations and powerful excitation sources as a result of low absorption coefficients in the Laporte forbidden f-f transitions that populate the Yb^{3+} excited state $^2F_{5/2}$.

When $[(YbL^1)_2Tb]$ is illuminated at 310 nm, photosensitisation by an antennae effect takes place through strong $\pi\rightarrow\pi^*$ absorption transitions of the bipyridyl units. This is followed by ET to the Yb^{3+} and Tb^{3+} centres and results in observation of both emissions corresponding to $^5D_4\rightarrow{}^7F_J$ (J=6 to 3) for Tb^{3+} as well as the 980 nm $^2F_{7/2}\rightarrow{}^2F_{5/2}$ for Yb^{3+}. Alternatively, when 980 nm radiation is supplied, cooperative photosensitisation UC occurs with ETU from 2 Yb^{3+} excited ions to Tb^{3+}, resulting in green and red emissions. This second route resembles that of the $SeCl_2$ host lattice doped with Yb:Tb mechanism. The QYs of $[(YbL^1)_2Tb]$ remain very low; ET efficiency from L^1 to Yb alone is 0.038, whilst the overall QYs in D_2O solution with $[(YbL_D)_2Tb_x]$ are only 10^{-8}-10^{-9}. Substantially increasing UC efficiency requires optimisation of the antenna effect.

In the case of $[(YbL^1)_2Tb]$, the wrapping of the L^1 around the Yb^{3+} results in a high negative charge density on one hemisphere of the complex. This allows polynuclear species, like $[(YbL^1)_2Tb_x]$, where x=1 to 3, to be formed.[2,3] Alternatively, $[(Yb(L^2))_2Tb]$ controls supramolecular assembly processes through strong electrostatic interactions between negatively charged Yb(tacn) and positively charged Tb in solution.[5] Within the frame of Forster's theory[5] of energy transfer, there is a $1/r^6$ distance dependence of the ET efficiency. In both cases, short distance donor/acceptor pairs are achieved by these electrostatic attraction of Yb complex and Tb cation.

$[(Yb(tacn))_2Tb]$, like $[(YbL^1)_2Tb]$, undergoes cooperative photosensitisation UC upon NIR excitation of Yb^{3+}, resulting in green emissions

of Tb^{3+} cations. Despite the Yb^{3+} being better shielded in $[(Yb(tacn))_2Tb]$, the activator Tb^{3+} is significantly more solvated than that in $[(YbL^1)_2Tb]$. Considering that cooperative sensitisation is phonon-assisted, O-D oscillators of the solvent D_2O may contribute to faster ET. This suggests that the more solvated Tb^{3+} in $[(Yb(tacn))_2Tb]$ will result in faster deactivation, hence shorter observed lifetime of 10.2 µs compared to 65 µs in $[(YbL^1)_2Tb]$. The Yb centred luminescence efficiency of $[(Yb(L^2))_2Tb]$ (ϕ_{D2O}=0.0075) is approximately 5-fold smaller compared to that of $[(YbL^1)_2Tb]$ (ϕ_{D2O}=0.0375).

Special Molecular Systems

The $[(Yb(L^2))_2Tb]$ complex is the only species able to luminesce in non-deuterated water at room temperature. The change from D_2O to water results in a decrease of the Tb emission intensity and lifetime due to vibrational energy transfer to the oscillators. This putative breakthrough can potentially be

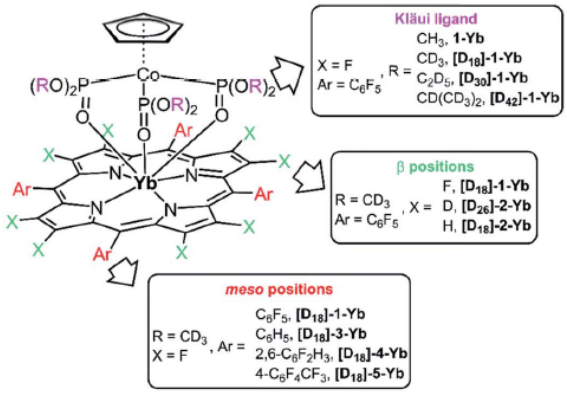

Figure 6: Sandwich structure showing an octafluorinated porphyrinate antenna ligand and deuterated Klaui ligand coordinated above the plane.[4]

used in the development of UC molecular probes for applications in bioanalytical technologies, once optimisation is achieved. Realistically, this complex can only have very niche applications, which may be too expensive to implement into bioanalytical technology. Additionally, the quantum yield of this UC device is too low (less than 10^{-9}, making the emission intensity difficult to measure) and the excitation energy too high to be applied to bioimaging.[9] The potential applications listed could, take place after extensive research on toxicity effects and studies on possible tissue compatibility has been done.

With the apparent exception of one discrete system (63 %)[4], no high sensitisation efficiencies have been reported for molecular systems, with particular difficulty in achieving large intrinsic quantum yields (approximately 12 %).[4] In the case of two octafluorinated phrophyrinate antenna ligands wrapped around the Yb^{3+} ion , capped by a deuterated Klaui ligand (*Figure 6*), a more effective antenna effect was reported, with a sensitisation efficiency close to 1.00 and an intrinsic quantum yield of 0.63.

Here, UC does not take place as only Yb^{3+} ions are present. Instead, the perfluorinated porphyrin acts as the sensitiser by harvesting light and transferring that energy to the Yb^{3+}, exciting it to $^2F_{5/2}$. Porphyrinates have an

intense visible light absorption and tunable triplet states above the excited state levels of NIR emissive Yb^{3+} ion, with an energy gap of 2000-3000 cm^{-1} resulting in high sensitisation efficiency and large intrinsic QY. In attempts to minimize quenching and non-radiative processes, fluorination and deuteration techniques are used as in the previous examples. Coordinating N and O atoms make up the primary coordination sphere, followed by porphyrinate and phosphito groups of Klaui in secondary and C-H oscillators of meso-phenyl groups in the tertiary sphere (with ortho quenching more than meta and para). Having already achieved such high quantum yields, further work can be done to alter the meso-phenyl groups of the β-octafluorinated porphyrins, enabling the design of further materials.

Dual-Mode Luminescence in Nanoparticles

In addition to the myriad of examples of solid and molecular state systems, that can undergo GSE followed by ETU, other systems with dual-mode long-lived luminescence also exist. These systems can undergo both up-conversion as well as down-conversion, depending on the irradiation and hence excitation taking place. One such example is that of a multilayer nanoparticle, $NaGdF_4$:Yb/Tm@$NaGdF_4$:Ce/ Mn@$NaYF_4$, with an Yb^{3+}/Tb^{3+} centre, Ce^{3+}/Mn^{2+} intermediate layer and Y^{3+} outer layer. During the UC mechanism, the core section harvests NIR excitation energy, through the Yb^{3+} $^2F_{7/2} \rightarrow {}^2F_{5/2}$ transition, in order to promote Gd^{3+} $^8S_{7/2} \rightarrow {}^6P_{7/2}$. Gd-sublattice-mediated energy migration occurs, where this excited energy then is trapped by the Mn^{2+} dopants in the middle layer. Alternatively, during the DC mechanism, the middle layer absorbs UV irradiation at 254 nm by exciting the Ce^{3+} ions. This excitation energy travels through the Gd^{3+} ion arrays to reach the same Mn^{2+} and resulting in the same green luminescence.[6]

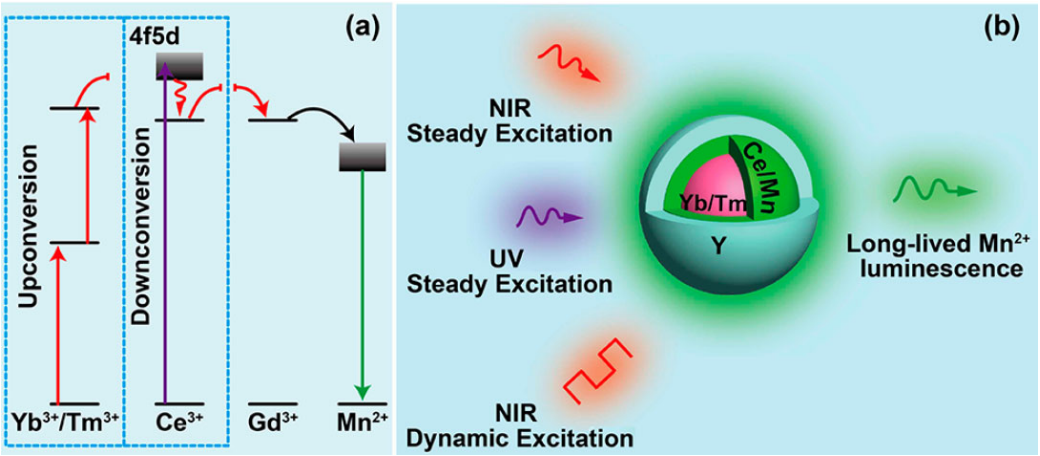

Figure 7: Proposed ET pathways for dual-mode luminescence of the same Mn^{2+} centre upon NIR (980 nm) and UV (254 nm) excitation, showing an idealised structure of the nanoparticle.[6]

In both the UC and DC, dual emissions are observed at the characteristic wavenumbers of Tm^{3+} (345, 368, 450, 477 and 650 nm) and a broad emission band at 531 nm attributed to $^4T_1 \rightarrow {}^6A_1$ of Mn^{2+}. The Mn^{2+} transition is spin-forbidden and is associated with a long-lived 32 ms luminescent lifetime, whereby the green emission is still visible after excitation at the other wavelengths has died away. In such multi-doped systems, the composition of every dopant affects the ET efficiencies and hence luminescence lifetimes. Through the introduction of Ce^{3+} ions in the middle layer, green DC emissions became visible from the same Mn^{2+} dopants upon 254 nm excitation (instead of 980 nm). However, if the Ce^{3+} concentration is too high, the ET efficiency of Gd^{3+} to Mn^{2+} drops, due to Gd^{3+} energy relay to both Ce^{3+} and Mn^{2+}.

Such Dual-system nanoparticles could potentially be used for data encoding and biolabeling. The outer surface of the nanoparticle is coated by $NaYF_4$ protective layer, where additional ligands can be added. This is promising in potential biolabeling applications, allowing for surface modification and bioconjugation procedures in identification of target proteins.[9] Additionally, long-lived Mn^{2+} luminescence theoretically enables ease of data decoding by cell phone cameras under burst mode.

Biolabeling and Luminescent Nanoparticles

UC Nanoparticles (UCNP) are particularly advantageous over conventional organic dyes markers and quantum dots.[9,10] The NIR excitation allows for deeper penetration into tissue due to lower scattering and tissue absorption at these wavelengths and has a much higher signal-to-noise ratio due to the absence of autofluorescence.[9,10]

In the case of $NaYF_4$:Yb,Er, the cytotoxicity in endothelial and liver cells are very low, whilst biocompatibility is high, without affecting cell morphology. With appropriate surface modification and bioconjugation procedures, these UCNPs can be taken into the cells and target specific proteins.[9] In order to increase cell uptake, particle aggregation must be minimized by controlling functionalized UCNP concentration. Individual UCNPs are observed inside cells, whereas aggregated particle clusters remain outside cells due to their size.[10] The UCNP within cells are predominantly found within the cytoplasm and none is in the nucleus.[9]

Cooperative UC takes place when 2 Yb^{3+} ions become excited, radiatively and cooperatively transfer that energy to Er^{3+}. The red emissions from Er^{3+} corresponds to $^4F_{9/2} \rightarrow {}^4I_{15/2}$, whilst the green emission corresponds to $^4S_{3/2}, {}^2H_{1/2} \rightarrow {}^4I_{15/2}$. The green emission is weaker in endothelial cells, resulting in an orange/red visible colour.[9] By comparison,

the red emission is quenched in liver tissue due to localized interactions between UCNPs and cellular proteins in the liver, giving a green emission.

White Light Up-Conversion

White light UC emissions and colour tunability can be achieved, in a similar way to how illuminating a multi-doped system with different irradiations leads to different mechanisms in the multilayer nanoparticle. The tridoped $Er^{3+}/Tm^{3+}/Yb^{3+}$ $YNbO_4$ phosphor system allows multicolour, like white light (red, green and blue), to be obtained by adjusting the relative Tm^{3+} and Yb^{3+} compositions.[7,8] The same multicolour, is observed when the system is irradiated with 980 nm, causing GSE of Yb^{3+} with $^2F_{7/2}\rightarrow{}^2F_{5/2}$ transition, or with 808 nm, causing the GSE of Er^{3+} with $^4I_{15/2}\rightarrow{}^4I_{9/2}$ or Tm^{3+} with $^3H_6\rightarrow{}^3H_4$ followed by a synergistic UC mechanism. Parallel to the changing in dopant concentrations in the multilayer nanoparticle system, such is the case with the concentrations of Er^{3+}, Yb^{3+} and Tm^{3+}. In the phosphor system, however, the blue light emitters are not as efficient as the green and red emitters. This is because only one transition corresponds to blue emissions, compared to numerous transitions corresponding to red and green emissions.

In the case of 980 nm excitation, Yb^{3+} acts as the sensitiser, because of its efficiency in ET to activator ions owing to large spectral overlap between Yb^{3+} emission ($^2F_{5/2}\rightarrow{}^2F_{7/2}$) and the absorption bands of Tm^{3+} ($^3H_6\rightarrow{}^3H_5$) and Er^{3+} ($^4I_{15/2}\rightarrow{}^4I_{11/2}$)). Red emissions are contributions from $^1G_4\rightarrow{}^3F_4$, $^3F_{2,3}\rightarrow{}^3H_6$ transitions of Tm^{3+} and $^4F_{9/2}\rightarrow{}^4I_{15/2}$ transitions of Er^{3+}, with Er^{3+} $^4F_{9/2}\rightarrow{}^4I_{15/2}$ transitions having a larger influence. The green emissions correspond to Er^{3+} $^2H_{11/2}$ or $^4S_{3/2}\rightarrow{}^4I_{15/2}$, whilst the blue only corresponds to Tm^{3+} $^1G_4\rightarrow{}^3H_6$. The red and green emissions correspond to a two-photon ETU process, whilst the blue corresponds to 3-photon ETU, competing with other UC processes like cross-relaxation, back energy transfer (BET) and saturation effect.

By comparing *Figures* 8 and 9, of the 808 nm and 980 nm excitations, the schemes involved are almost identical. In both cases, there are a large number of competing mechanisms, as well as, the same cross relaxations and back energy transfers. The main differences in the 808 nm irradiation include the GSA of Er^{3+} or Tm^{3+} which are replaced by GSA of Yb^{3+} in 980 nm radiation, due to the low luminescent efficiency of Er^{3+} or Tm^{3+}. Additionally, there are 2 ESA present in 808 nm illumination, which are absent at 980 as these are outcompeted by the Yb^{3+} excitation. This tri-doped system has potential application in different lighting technologies, like field colour displays, UC laser and white light sources.

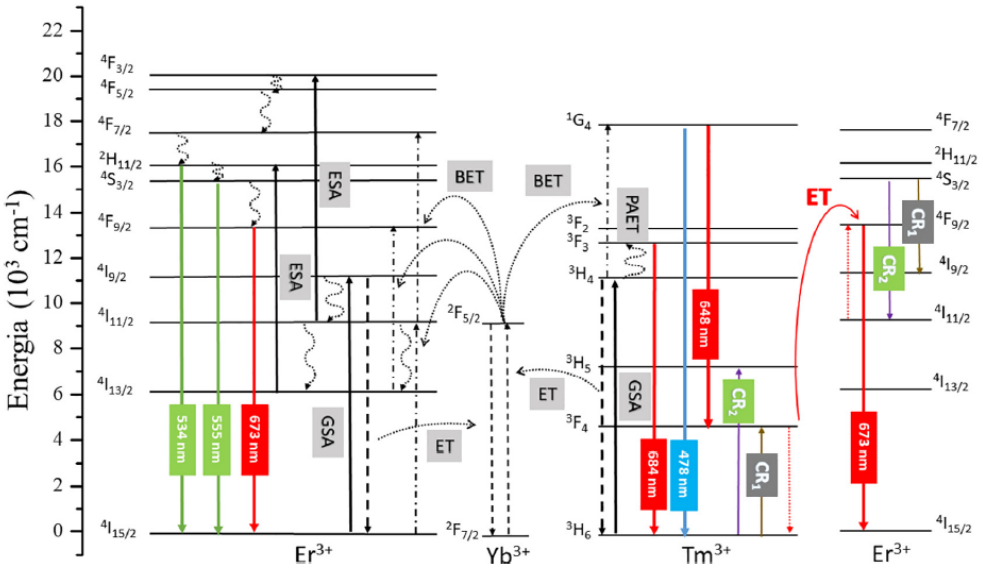

Figure 8: Energy level diagram for proposed UC mechanism of Er^{3+}, Yb^{3+} and Tm^{3+}, upon 808 nm excitation.[8]

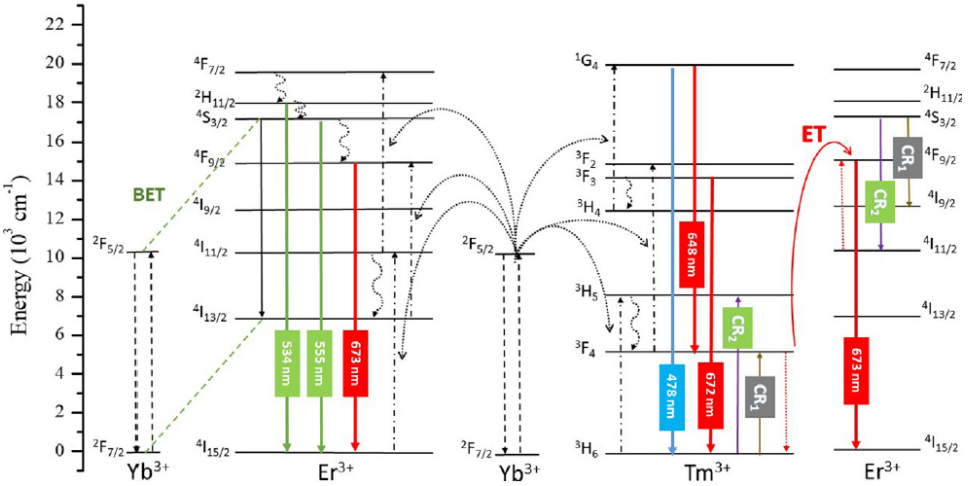

Figure 9: Energy level diagram for proposed UC mechanism of Er^{3+}, Yb^{3+} and Tm^{3+}, upon 980 nm excitation.[7]

Conclusions

In summary, the main issues affecting UC luminescence efficiency include quenching through high lattice phonon energies in host lattices, high vibrational oscillators and localized interactions with proteins. These different interactions quench different excited state species in the photophysical pathway and hence result in different luminescent colours being observed.

Systems that can undergo UC various potential applications, stretching from security,[6] biolabeling[9,10] and cell phone devices.[6] The UC luminescence achieved in non-deuterated water at room temperature represents a milestone in spectroscopy. Practically UC in solutions has limited

applications due to high excitation energy required and low QY achieved. Theoretically, these QYs could be improved by using systems containing the Klaui and porphyrinate antennae, but the cost to implement such systems to bioanalytical technologies would still be very high. Moreover, the analysis of biosystems requires a narrow spectral window in which to operate, which may not match with the new discrete molecular systems or dual-mode nanoparticles.

Furthermore, other advances could include additional multi-colours observed through excitation at 980 nm and 808 nm, potentially leading to backlight and white light sources. These systems need to be cheap in order to be commercially available and replace existing blacklight and white-light sources, rendering them impractical for the near future.

References:

1. G. M. Salley, R. Valiente and H. U. Güdel, *J. Phys.: Condens. Matter,* 2002, **14**, 5461
2. N. Souri, P. Tian, C. P. Iglesias, K. L. Wong, A. Nonat, L. J. Charbonniere, *J. Am. Chem. Soc.,* 2017, 139, **4**, 1456-1459
3. L. J. Charbonniere, *Dalton Trans.*, 2018, **47**, 8566
4. J.Y. Hu, Y. Ning, Y. Meng, J. Zhang, Z. Wu, *Chem. Sci.*, 2017, **8**, 2702
5. A. Nonat, S. Bahamyirou, A. Lecointre, F. Przybilla, Y. Mély, *J. Am. Chem. Soc.,* 2019, **141**, 1568−1576
6. X. Liu, Q. Ji, Q. Hu, C. Li, M. Chen, J. Sun, Y. Wang, Q. Sun, B. Geng, *ACS Appl. Mater. Interfaces,* 2019, **11**, 30146−30153
7. Felipe F. do Carmoa, João P.C. do Nascimentoa,b, Marcello X. Façanhaa,b,c, T.O. Salesd, W.Q. Santosd, Artur S. Gouveia-Netod, Carlos Jacintod, Antonio S.B. Sombrab, *J. Lumin.*, 2018, **204**, 676-684
8. Felipe F. do Carmo, João P.C. do Nascimento, Marcello X. Façanha, Antonio S.B. Sombra, *Mater. Lett.*, 2019, **254**, 65-68
9. Nampi, Padmaja Parameswaran, Vakurov, Alexandre, Mackenzie, Lewis E., Scrutton, Nigel S., Millner, Paul A., Jose, Gin, Saha, Sikha, *J. Biophotonics*, 2019, **12**,4
10. J. Shan, J. Chen, J. Meng, J. Collins, W. Soboyejo, J. S. Friedberg, Y. Ju, *J. Appl. Phys.*, **2008**, 104